Vacuum decay induced by quantum fluctuations

Haiyun Huang[*] and L. H. Ford[†]

Institute of Cosmology, Department of Physics and Astronomy Tufts University, Medford, Massachusetts 02155, USA

(Received 19 May 2020; accepted 7 April 2022; published 29 April 2022)

We treat the effects of quantum field fluctuations on the decay of a metastable state of a self-coupled scalar field. We consider two varieties of field fluctuations and their potential effects in a semiclassical description. The first are the fluctuations of the time derivative of a free massive scalar field operator, which has been averaged over finite regions of space and time. These fluctuations obey a Gaussian probability distribution. A sufficiently large fluctuation is assumed to produce an effect analogous to a classical initial field velocity, which can cause a finite region to fly over the barrier separating the metastable state from the stable vacuum state. Here we find a contribution to the decay rate which can be comparable to the decay rate by quantum tunneling, as computed in an instanton approximation. This result is consistent with those of other authors. We next consider the effects of the fluctuations of operators which are quadratic in the time derivative of the free scalar field. The quadratic operator is also averaged over finite regions of space and of time. Now the probability distribution for the averaged operator falls more slowly than an exponential function, allowing for the possibility of very large fluctuations. We find a contribution to the decay rate which, under certain conditions, may be larger than those coming from either quantum tunneling or linear field fluctuations.

DOI: 10.1103/PhysRevD.105.085025

I. INTRODUCTION

Quantum tunneling is a well-known effect in quantum mechanics. For example, a quantum particle in a local potential minimum has a nonzero probability to tunnel through a potential maximum to reach another potential minimum with lower energy. In many cases, the tunneling amplitude may be accurately calculated using the WKB approximation. However, there can be quantum field theoretic corrections to the tunneling rate calculated in single particle quantum mechanics. If the particle has an electric charge, it will respond to vacuum fluctuations of the electric field, which will result in a small increase in the tunneling rate [1,2]. This increase arises from a one-loop correction to the tree level scattering amplitude, which here could be the WKB tunneling amplitude. If the particle is an electron, then this correction is described by the one-loop vertex diagram in quantum electrodynamics. However, as was discussed in Ref. [2], the increase in tunneling rate may be reasonably estimated from a simple semiclassical argument. The particle is subjected to vacuum electric field fluctuations even if no real photons are present. These fluctuations exert a force on the particle which can either push the particle toward the barrier, enhancing the tunneling probability, or away from the barrier, suppressing tunneling. However, the average effect is a small enhancement of the tunneling rate, in agreement with the one-loop perturbation theory calculation.

Vacuum radiation pressure fluctuations can also enhance the transition rate, and were studied in Ref. [3]. Here the enhancement is potentially larger, and can possibly dominate over the effect predicted by the WKB approximation. This type of large vacuum fluctuation will be discussed in more detail below in Sec. V. Vacuum radiation pressure fluctuations on Rydberg atoms were recently discussed in Ref. [4], where it was argued that these fluctuations might produce observable effects.

The topic of the present paper will be role of quantum field fluctuations in the decay of a false vacuum state in field theory. Consider a real scalar field, $\phi(\mathbf{x}, t)$, with self-coupling described by a potential, $U(\phi)$, which has at least two local minima. If we quantize small perturbations around the global minimum, the ground state of the resulting field theory is called the true vacuum, whereas if we select a minimum with higher energy, the corresponding state is called a false vacuum, and is potentially unstable against decay into the true vacuum. A Euclidean space formalism which describes this decay by quantum tunneling was developed by Coleman [5], and will be reviewed in Sec. II.

[*]jasmine.haiyun@gmail.com
[†]ford@cosmos.phy.tufts.edu

Published by the American Physical Society under the terms of the Creative Commons Attribution 4.0 International license. Further distribution of this work must maintain attribution to the author(s) and the published article's title, journal citation, and DOI. Funded by SCOAP[3].

The outline of this paper is as follows: Section II will review false vacuum decay by quantum tunneling, as described in the instanton approximation. Section III will discuss the classical dynamics of a self-coupled scalar field with two local potential minima, and illustrate how suitable initial conditions on the time derivative, $\dot{\phi}$, of the classical field can cause a finite region to fly over the potential maximum separating these minima. In Sec. IV, we consider the effects of the vacuum fluctuations of the linear field operator, $\dot{\phi}(\mathbf{x}, t)$, averaged over a finite spacetime region, and argue that this effect can be of the same order as the instanton contribution to the decay rate. A similar conclusion was reached some time ago by Linde [6], who studied the effects of ϕ fluctuations in de Sitter spacetime. The effects of linear field fluctuations were also studied by Calzetta, Verdaguer, and coworkers [7–11] in several models, and agree with Linde's conclusion. After an early version of our results was first presented [12], we become aware of the recent work of several authors [13–16], who treat either ϕ or $\dot{\phi}$ fluctuations in either Minkowski or de Sitter spacetime, and also conclude that the contribution to the decay rate is of the same order as the instanton contribution. However, these authors disagree as to whether linear quantum field fluctuations and instanton methods are different formalisms for describing the same physical process, or whether they describe physically distinct processes. This is a question to which we will return later in this paper. Section V will discuss the fluctuations of a spacetime average of the quadratic operator $\dot{\phi}^2$. We first review results from Refs. [17–21] to the effect that the probability distribution for such an operator can fall more slowly than an exponential function. We then discuss whether the effects of $\dot{\phi}^2$ fluctuations on the decay rate of the false vacuum can be larger than either quantum tunneling, as described by an instanton, or the effects of linear field fluctuations. Our results are summarized and discussed in Sec. VI.

Units in which $\hbar = c = 1$ will be used throughout this paper.

II. INSTANTON METHODS

The instanton method approximates a path integral in Euclidean space as being dominated by one or more solutions of locally minimum Euclidean action, the instantons. This leads to an expression for a transition amplitude in the form of a sum of terms of the form $\exp(-S)$, where S is the Euclidean action of an instanton. This method is analogous to the use of the saddle point or stationary phase approximations for the evaluation of ordinary integrals, and is reviewed by Coleman in Ref. [22].

A. Quantum mechanics and the Schwinger effect

Instanton methods may be used to compute barrier tunneling rates in single particle quantum mechanics. The results are similar to those from the WKB approximation. The instanton and WKB methods have been compared by several authors [23–25], who find that the two methods are not identical, but often give answers which agree to reasonable accuracy.

Instanton methods may also be applied to the Schwinger effect [26], the creation of pairs of charged particles and antiparicles from the vacuum by a constant electric field. This was done by Garriga [27] both in a $1+1$ and in a $3+1$ dimensional models. The $3+1$ dimensional case was treated in more detail by Kim and Page [28]. The result for the creation rate obtained by instanton approaches agree with those found by Bogolubov coefficient methods in $1+1$ [29] and in $3+1$ dimensions [30], as well as with Schwinger's original approach using an effective action. Thus the instanton approach seems to give a reliable description of the Schwinger effect.

B. Instantons in quantum field theory and false vacuum decay

In this section, we summarize the instanton method used by Coleman [5] to estimate the rate of false vacuum decay. Consider a real scalar field with the Lagrangian density

$$\mathcal{L} = \frac{1}{2}\partial_\mu\phi\partial^\mu\phi + U(\phi), \tag{2.1}$$

where $U(\phi)$ is a "double well" potential with two minima. The associated equation for $\phi(\mathbf{x}, t)$ is

$$\Box\phi - U'(\phi) = 0, \tag{2.2}$$

where $\Box$ denotes the d'Alembertian operator in Lorentzian space [where we use metric signature $(-,+,+,+)$], and the four-dimensional Laplacian in Euclidean space. A specific choice for $U(\phi)$ is

$$U(\phi) = \frac{\lambda}{8}(\phi^2 - a^2)^2 + \frac{\epsilon\lambda a^3}{2}(\phi - a), \tag{2.3}$$

where λ, a, and ϵ are positive real constants. This form is illustrated in Fig. 1 for the case

$$\lambda = 0.01, \qquad a = 1000, \qquad \epsilon = 0.1. \tag{2.4}$$

The potential has a local minimum at $\phi = \phi_+$, the false vacuum, and a global minimum at $\phi = \phi_-$, the true vacuum. These minima are separated by a local maximum at $\phi = \phi_m$. The potential difference between the false vacuum and the local maximum is $\Delta U = U(\phi_m) - U(\phi_+)$. For the choice of parameters given in Eq. (2.4) and illustrated in Fig. 1, $\phi_- \approx -1046.7$, $\phi_m \approx 101.0$, and $\phi_+ \approx 945.6$. Thus

$$\Delta\phi = \phi_+ - \phi_m \approx 845 \quad \text{and} \quad \Delta U \approx 7.88 \times 10^8, \tag{2.5}$$

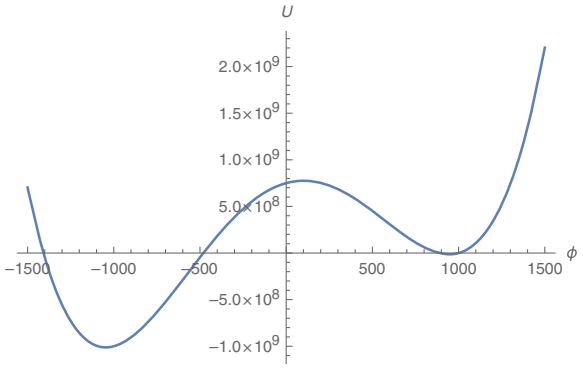

FIG. 1. The potential $U(\phi)$ given in Eq. (2.3) is plotted with the choice of parameters in Eq. (2.4).

quantities which will be used later. In the vicinity of the false vacuum, ϕ is approximately a free massive scalar field of mass m, and $U(\phi)$ has the form

$$U(\phi) \approx U(\phi_+) + \frac{1}{2}m^2(\phi-\phi_+)^2 + O[(\phi-\phi_+)^3]. \quad (2.6)$$

For small ϵ, we have the estimate

$$m \approx a\sqrt{\lambda}. \quad (2.7)$$

For the parameters given in Eq. (2.4), a more precise value is

$$m \approx 91.7267. \quad (2.8)$$

If the system is initially in the false vacuum state, we expect it to be unstable to decay to the true vacuum. In principle, the decay probability may be computed in the path integral formalism as

$$P \sim \sum_{\phi(x)} \exp(-S_E[\phi]), \quad (2.9)$$

where $\phi(x)$ is a field configuration in Euclidean space which approaches both ϕ_+ and ϕ_- in different limits. Here S_E is the Euclidean action, given by

$$S_E[\phi] = \int dt_E d\vec{x}\left[\frac{1}{2}\left(\frac{\partial\phi}{\partial t_E}\right)^2 + \frac{1}{2}(\vec{\nabla}\phi)^2 + U\right], \quad (2.10)$$

where the Wick rotation $t_E = it$ has been performed. The summation in Eq. (2.9) requires a sum over configurations $\phi(x)$, which cannot be computed exactly by any known methods. The instanton approximation assumes that this sum is dominated by solutions of the Euclidean version of Eq. (2.2) near that with the lowest Euclidean action. Coleman calls this the "bounce" solution, for which $S_E = B$. In the instanton approximation, the decay probability becomes

$$P \propto e^{-B}, \quad (2.11)$$

or specifically we can write the decay rate per unit volume as

$$\Gamma_I \approx Ke^{-B}. \quad (2.12)$$

The prefactor K is treated by Callan and Coleman [31], who show that it may be expressed as a functional determinant which has the dimensions of the reciprocal of the product of time and volume, so that Eq. (2.12) may be interpreted as a rate per unit spatial volume.

The bounce solution is assumed to be $O(4)$ symmetric, and hence Eq. (2.2) becomes an ordinary differential equation with independent variable $\rho = (t_E^2 + |\mathbf{x}|^2)^{1/2}$, the radius in four-dimensional Euclidean space. Here $t_E = it$ is the Euclidean time. This equation can be integrated numerically. We do this using the software package described in Ref. [32]. The result for the case of the parameters given in Eq. (2.4) is illustrated in Fig. 2. This solution describes the nucleation of a bubble filled with the true vacuum, which nucleates in the false vacuum with an initial radius of $\rho = \rho_0 \approx 0.2$. The bounce action in this case is

$$B \approx 2.47 \times 10^6. \quad (2.13)$$

The function $\phi(\rho)$ describes the spatial configuration of the bubble when it nucleates, with ϕ varying from the false vacuum value in the interior of the bubble to the true vacuum value on the exterior. The wall of the bubble is the region where ϕ varies most rapidly with increasing ρ. After nucleation, the bubble expands, with ρ taking the Lorentzian form, $\rho = (|\mathbf{x}|^2 - t^2)^{1/2}$. Thus the expansion of the wall of the bubble is described by a spacetime hyperbola, which is the world line of a uniformly accelerated particle. The expansion requires that the volume energy on the interior of the bubble at least balance the surface energy in the wall. As the bubble expands, the

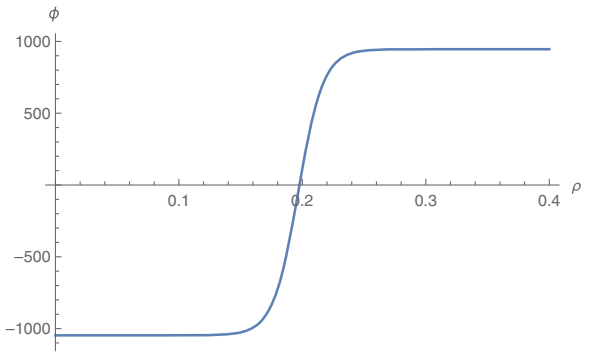

FIG. 2. The bounce solution $\phi(\rho)$ for the potential given in Eq. (2.3) with the choice of parameters in Eq. (2.4). Here $\phi(0) = \phi_-$ and $\phi(\rho) \to \phi_+$ as $\rho \to \infty$.

volume energy decreases due to the lower energy density of the true vacuum relative to the false vacuum, while the surface energy arising from spatial gradients in the wall increases. Bubbles with radii less than the minimum value, ρ_0, will collapse rather than expand. This is similar to nucleation of bubbles of vapor in a boiling liquid.

There is one limit in which the bounce solution may be obtained analytically, when $\epsilon \ll 1$. This case, called the thin-wall approximation, is treated in Sec. IV of Ref. [5]. However, there seem to be a few numerical errors in this reference. We find that there should be an additional factor of 2 on the right-hand side of Eq. (4.12), which leads to an additional factor of 16 on the right-hand side of Eq. (4.21) of Ref. [5]. There also appear to be a factor of 2 missing from the last term of Eq. (4.15), but this is corrected in the following expression, Eq. (4.16). Note that the parameter ϵ is defined differently in Ref. [5] from our definition. There the potential is written in the form

$$U(\phi) = \frac{\lambda}{8}(\phi^2 - a^2)^2 + \frac{\epsilon_1}{2a}(\phi - a), \tag{2.14}$$

where $\epsilon_1 = \epsilon\lambda a^4$, when ϵ is defined as in Eq. (2.3). Accounting for both these corrections, and the change in notation, the initial radius of the bubble becomes

$$\rho_{0tw} = \frac{2}{\epsilon a\sqrt{\lambda}}, \tag{2.15}$$

and the bounce action is

$$B_{tw} = \frac{8\pi^2}{3\epsilon^3\lambda}. \tag{2.16}$$

The above corrections seem to be consistent with the results of Garbrecht and Millington [33], who write the potential in the form

$$U = \frac{\lambda_1}{4!}\Phi^4 + \frac{g}{6}\Phi^3 - \frac{1}{2}m_\Phi^2\Phi^2 + U_0. \tag{2.17}$$

This form is equivalent to Eq. (2.3), as may be seen by letting $\Phi = \phi + s$ and expanding Eq. (2.17) to find

$$\lambda = \frac{1}{3}\lambda_1, \tag{2.18}$$

$$s = -\frac{g}{\lambda_1}, \tag{2.19}$$

$$a^2 = \frac{3}{\lambda_1^2}(2m_\Phi^2\lambda_1 + g^2) \approx \frac{6m_\Phi^2}{\lambda_1} + O(g^2), \tag{2.20}$$

and

$$\epsilon = 2g\frac{3m_\Phi^2\lambda_1 + g^2}{3^{3/2}(2m_\Phi^2\lambda_1 + g^2)^{3/2}} \approx \frac{g}{\sqrt{6\lambda_1}m_\Phi} + O(g^2). \tag{2.21}$$

Note in Eqs. (2.20) and (2.21), we have given an expansion to first order in g, which reveals that $g \ll \sqrt{\lambda_1}m_\Phi$ is equivalent to $\epsilon \ll 1$, the thin wall approximation. We may use the above expressions to show that Eq. (2.15) and Eq. (2.16) are equivalent to the corresponding results given by Garbrecht and Millington in Eqs. (12) and (13), respectively, of Ref. [33].

As noted above, Callan and Coleman [31] express the prefactor K in Eq. (2.12) as a functional integral which is difficult to calculate explicitly in general. However, it may be found explicitly in the thin wall approximation from a functional integration over zero modes, which was done by subsequent authors, including Garbrecht and Millington [33]. The result in the latter reference may be expressed as

$$K \approx \frac{32\pi^2}{9\sqrt{3}}\epsilon^{-7}a^4[1 + O(\epsilon^2)]. \tag{2.22}$$

Recall that ϵ and λ are dimensionless constants, but that a has dimensions of $1/\text{time} = 1/\text{length}$, so K has the correct dimensions for a rate per unit volume. Note that $K \propto \epsilon^{-7}$ is very large in the thin wall limit, but the decay rate given by Eq. (2.12) vanishes as $\epsilon \to 0$ due to the fact that $B_{tw} \propto \epsilon^{-3}$ appears in the exponential.

III. CLASSICAL FIELD DYNAMICS

A. Energy conservation

Consider a real classical field ϕ which satisfies the equation of motion Eq. (2.2) in Minkowski spacetime, so

$$\Box\phi = -\partial_t^2\phi + \nabla^2\phi = U'(\phi). \tag{3.1}$$

The associated energy density of this field is

$$T_{tt} = \frac{1}{2}[(\partial_t\phi)^2 + |\boldsymbol{\nabla}\phi|^2] + U(\phi). \tag{3.2}$$

Consider a finite spatial region R, and define the field energy in this region at time t by

$$E_R(t) = \int_R d^3x T_{tt}(\mathbf{x}, t). \tag{3.3}$$

Then

$$\begin{aligned}\frac{dE_R}{dt} &= \int_R d^3x\{\partial_t\phi[\partial_t^2\phi + U'(\phi)] + \boldsymbol{\nabla}\phi\cdot\boldsymbol{\nabla}\partial_t\phi\} \\ &= \int_R d^3x\{\partial_t\phi[\partial_t^2\phi - \nabla^2\phi + U'(\phi)] + \boldsymbol{\nabla}\cdot(\partial_t\phi\boldsymbol{\nabla}\phi)\}.\end{aligned} \tag{3.4}$$

The last term in the above expression is a total divergence, which may be written as a surface integral over the boundary S of region R:

$$\int_R d^3x \boldsymbol{\nabla}\cdot(\partial_t\phi\boldsymbol{\nabla}\phi) = \oint_S d\mathbf{S}\cdot(\partial_t\phi\boldsymbol{\nabla}\phi), \tag{3.5}$$

which will vanish if either $\partial_t\phi$ or the normal component of $\boldsymbol{\nabla}\phi$ vanish on each point of S. In this case, Eqs. (3.1) and (3.4) imply that E_R is a constant.

In the case of a spatially homogeneous field, $\phi = \phi(t)$, the spatial integration simply produces a constant factor of the volume of R, and $E_R \propto (\dot{\phi})^2/2 + U(\phi(t))$. This is of the same form as the energy of a point particle in a potential. The turning points of the motion occur when $U(\phi)$ reaches its maximum value, and $\dot{\phi} = 0$. The case of an inhomogeneous field is somewhat more complicated, but one can still approximately identify turning points as occurring when $\int_R d^3x U(\phi(t)) \approx E_R$, when the contributions of both $(\dot{\phi})^2$ and $|\boldsymbol{\nabla}\phi|^2$ to E_R are small. Thus if the variation of ϕ within R is small compared to the variation between a pair of turning points of $U(\phi)$, we can view R as a localized region which moves between these turning points much as does a point particle.

B. Motion over a barrier

Consider the dynamics of a finite region in a potential with local minima, such as illustrated in Fig. 1. If the energy E_R of the region is small, then the motion is expected to be confined to be near one minimum, analogous to that of a classical particle oscillating about a minimum. However, larger values of E_R might allow the region to pass over the local maximum. One way to achieve this would be to impose initial conditions that $\phi = \phi_+$, so the system starts in the false vacuum, and $\dot{\phi} = \dot{\phi}_0 \neq 0$ in a finite spatial region R. If $|\dot{\phi}_0|$ and the size of R are sufficiently large, then this region can move over the local maximum at ϕ_m to the global minimum at $\phi = \phi_-$. In the potential illustrated in Fig. 1, this can happen more easily if $\dot{\phi}_0 < 0$. This would be a classical version of quantum false vacuum decay. The region R becomes a bubble similar to those discussed in Sec. II. Again, there is a competition between the volume energy inside the bubble and surface energy in the wall, which requires that the bubble has a minimum size before it can expand rather than collapse. If the bubble does expand, it eventually fills all of space with a region where $\phi \approx \phi_-$, the global minimum. This will be illustrated in some numerical simulations in Sec. IV C 2. In the next section, we discuss a model where the classical initial condition on $\dot{\phi}_0$ is replaced by the effect of a quantum field fluctuation.

IV. VACUUM DECAY INDUCED BY $\dot{\phi}$ FLUCTUATIONS

In this section, we will be concerned with possible effects of the quantum fluctuations of the scalar field, ϕ, and its space and time derivatives, such as $\dot{\phi}$. We assume that initially $\phi \approx \phi_+$, the false vacuum value, and that to leading order, ϕ is a linear quantum field with mass m.

A. The probability distribution for spacetime averaged $\dot{\phi}$ fluctuations

The fluctuations of a field operator at a single spacetime point are not meaningful, but averages over space and/or time are well defined. We can view these averages as the result of a measurement of the field in a finite region. Here we consider averaging over both space and time regions and write the average of $\dot{\phi}$ as

$$\bar{\dot{\phi}} = \int dt\, f(t) \int d^3x\, g(\mathbf{x})\dot{\phi}(\mathbf{x}, t), \tag{4.1}$$

where the averaging functions are normalized by

$$\int dt\, f(t) = \int d^3x\, g(\mathbf{x}) = 1. \tag{4.2}$$

The probability distribution for $\bar{\dot{\phi}}$ fluctuations in the vacuum state is a Gaussian function,

$$P(\bar{\dot{\phi}}) = \frac{1}{\sqrt{2\pi\sigma^2}}\exp\left(-\frac{\bar{\dot{\phi}}^2}{2\sigma^2}\right), \tag{4.3}$$

where the variance σ^2 is

$$\sigma^2 = \langle\bar{\dot{\phi}}^2\rangle = \langle 0|\int dt_1 d^3x_1 f(t_1)g(\mathbf{x}_1)\dot{\phi}(t_1,\mathbf{x}_1) \times \int dt_2\, d^3x_2 f(t_2)g(\mathbf{x}_2)\dot{\phi}(t_2,\mathbf{x}_2)|0\rangle. \tag{4.4}$$

We may write the linear operator $\dot{\phi}$ as

$$\dot{\phi}(x) = \sum_{\mathbf{k}}\sqrt{\frac{\omega}{2V}}[e^{i(\mathbf{k}\cdot\mathbf{x}-\omega t)}a_k + e^{-i(\mathbf{k}\cdot\mathbf{x}-\omega t)}a_k^\dagger], \tag{4.5}$$

where V is a quantization volume, and $\omega^2 = k^2 + m^2$. In the large volume limit, this leads to an expression for the variance:

$$\sigma^2 = \frac{1}{2(2\pi)^3}\int d^3k\,\omega\hat{g}^2(\mathbf{k})\hat{f}^2(\omega), \tag{4.6}$$

where $\hat{f}(\omega)$ and $\hat{g}(\mathbf{k})$ are the Fourier transforms of the time and space sampling functions, respectively. We assume that $\tau \neq 0$ is the characteristic width of $f(t)$, and hence is the

time sampling interval. Similarly, let $\ell \neq 0$ be the characteristic spatial sampling interval. It is convenient to define dimensionless functions with unit sampling intervals by

$$f_1(t) = \frac{1}{\tau} f\left(\frac{t}{\tau}\right), \qquad g_1(\mathbf{x}) = \frac{1}{\ell^3} g\left(\frac{\mathbf{x}}{\ell}\right). \tag{4.7}$$

Let $\hat{f}_1$ and $\hat{g}_1$ be their corresponding Fourier transforms. We can now express the variance as

$$\sigma^2 = \frac{\eta}{2\ell^3 \tau}, \tag{4.8}$$

where

$$\eta := \frac{1}{(2\pi)^3} \int d^3\kappa \, \Omega \hat{g}_1^2(\boldsymbol{\kappa}) \hat{f}_1^2(\Omega), \tag{4.9}$$

with $\Omega^2 = \kappa^2 \frac{\tau^2}{\ell^2} + m^2\tau^2$. Note that η is a dimensionless quantity which depends upon the functional forms of the sampling functions, as well as any two of the three dimensionless variables $m\tau$, $m\ell$, and ℓ/τ.

In the limit where the mass vanishes, $m = 0$, we are left with two parameters, ℓ and τ. However, the variance σ^2, will be finite with either time averaging alone or spatial averaging alone. Thus we expect to have

$$\sigma^2 \propto \tau^{-4}, \qquad \tau \gtrsim \ell, \tag{4.10}$$

or

$$\sigma^2 \propto \ell^{-4}, \qquad \ell \gtrsim \tau. \tag{4.11}$$

Both of these limits are consistent with Eq. (4.8). When $\tau \gtrsim \ell$, we expect $\eta \propto (\ell/\tau)^3$, but that $\eta \propto \tau/\ell$ when $\ell \gtrsim \tau$.

Often we are interested in the probability of a fluctuation which exceeds a given threshold. Let $P(x)$ be a probability distribution, so that $\int_{x_0}^{x_1} P(x)dx$ is the probability of finding $x_0 \leq x \leq x_1$ in a given measurement. Define the complementary cumulative probability by

$$P_>(y) = \int_y^\infty P(x)dx. \tag{4.12}$$

This is the probability of finding $x \geq y$ in a given measurement. In the case where $P(x)$ is a Gaussian, such as given in Eq. (4.3) with $x = \bar{\dot{\phi}}$, $P_>(y)$ is expressible as an error function. For a large argument, it has the asymptotic form

$$\begin{aligned} P_>(y) &\sim \frac{\sigma}{\sqrt{2\pi}} \exp\left[-\frac{y^2}{2\sigma^2}\right]\left(\frac{1}{y} + O(y^{-2})\right) \\ &\approx \exp\left[-\frac{y^2}{2\sigma^2} - \ln(\sqrt{2\pi}y/\sigma)\right]. \end{aligned} \tag{4.13}$$

Thus if y is large enough that the logarithm term may be neglected, then $P_>(y)$ has approximately the same functional form as does $P(x)$.

B. Compactly supported functions

We adopt the view that the sampling functions $f(t)$ and $g(\mathbf{x})$ should have compact support, meaning that they are strictly equal to zero outside of finite intervals. The physical motivation for this is that these functions should describe measurements made within finite time intervals and spatial regions. A temporal sampling function such as a Gaussian or Lorentzian has tails which extend into the past and the future, and strictly describes a measurement which began in the infinite past and continues into the infinite future. A better choice is an infinitely differentiable function with compact support. Such functions have Fourier transforms which fall faster than any power, but more slowly than an exponential function. A class of these functions was discussed in Refs. [18,20], and have Fourier transforms with the asymptotic forms

$$\hat{f}(\omega) \sim \exp[-(\omega\tau)^\alpha], \qquad \omega\tau \gg 1, \qquad \hat{g}(k) \sim \exp[-(k\ell)^\lambda], \quad k\ell \gg 1, \tag{4.14}$$

where α and λ are real constants which satisfy $0 < \lambda \leq \alpha < 1$. Here the spatial sampling function is assumed to be spherically symmetric, so $g = g(r)$ and $\hat{g} = \hat{g}(k)$. The coordinate space switch-on or switch-off behavior is linked to the values of α and λ. For example, if $f(t)$ switches on at $t = 0$, then it might have the form

$$f(t) \sim D t^{-\mu} \exp(-w t^{-\nu}) \tag{4.15}$$

as $t \to 0^+$ for some constants D, μ, w, and ν. The most important of these is ν, which is related to the parameter α in $\hat{f}$ by $\nu = \alpha/(1-\alpha)$. The choice $\alpha = 1/2$, where $\nu = 1$, has special physical interest, as there is an electrical circuit which switches on with this behavior [18]. Some explicit examples of compactly supported functions were given in Sec. II B of Ref. [18] and in Appendix A of Ref. [20].

Another choice can be given in coordinate space by

$$f_1(t) = C_f \begin{cases} \exp\left(-\frac{1}{1-t^2}\right), & t \in [-1,1] \\ 0, & t < -1 \quad \text{or} \quad t > 1 \end{cases} \tag{4.16}$$

and

$$g_1(\vec{x}) = C_g \begin{cases} \exp\left(-\frac{1}{1-|\vec{x}|^2}\right), & |\vec{x}| \in [0,1] \\ 0, & |\vec{x}| > 1, \end{cases} \tag{4.17}$$

where C_f and C_g are normalization factors chosen so that Eq. (4.2) holds. The functions above correspond to $\alpha = \lambda = 1/2$, and $\tau = \ell = 1$.

C. Effects of large $\bar{\dot{\phi}}$ fluctuations

Let us return to the process described in Sec. III B, where a classical initial condition on $\dot{\phi}$ could cause a finite spatial region to move from the false vacuum, over the barrier to the true vacuum. However, we now consider quantum vacuum fluctuation of a space and time average, $\bar{\dot{\phi}}$, and ask under what conditions it might produce the same effect. The probability of a sufficiently large fluctuation may be estimated from Eqs. (4.3) and (4.8) once we have estimates for $\bar{\dot{\phi}}$, τ, ℓ, and η. We expect that we need $\frac{1}{2}\bar{\dot{\phi}}^2 \gtrsim \Delta U$, where

$$\Delta U = U(\phi_0) - U(\phi_F) \tag{4.18}$$

is the height of the potential barrier above the false vacuum level. Take the minimum value of the magnitude of $\bar{\dot{\phi}}$ to be

$$|\dot{\phi}_0| = (2\Delta U)^{\frac{1}{2}}. \tag{4.19}$$

Let the minimum value of τ be

$$\tau_0 = \frac{\Delta\phi}{|\dot{\phi}_0|}, \tag{4.20}$$

where $\Delta\phi = |\phi_0 - \phi_F|$. That is, τ_0 is the time that would be required for the field to change by $\Delta\phi$ if it maintained an average speed of $\dot{\phi}_0$. Finally, we estimate that the minimum size of the spatial averaging region should be of the order of the radius at which a bubble could nucleate in the given potential, in the thin wall approximation,

$$\ell_0 = \rho_{0tw}. \tag{4.21}$$

Recall that this is the minimum radius at which the internal pressure can balance the tension in the bubble wall. More generally, we expect the values of $\dot{\phi}$, τ, and ℓ to be of the order of the minimum values estimated above. Set

$$\dot{\phi} = V\dot{\phi}_0, \qquad \tau = T\tau_0, \qquad \ell = L\ell_0, \tag{4.22}$$

where V, T, and L are constants of order unity.

Let

$$A = \frac{\bar{\dot{\phi}}^2\ell^3\tau}{\eta} = V^2L^3T\frac{\bar{\dot{\phi}}_0^{\,2}\ell_0^3\tau_0}{\eta}. \tag{4.23}$$

The probability of a $\bar{\dot{\phi}}$-fluctuation which is sufficiently large to move a region over the potential barrier is of order

$$P(\bar{\dot{\phi}}) \approx P_>(\bar{\dot{\phi}}) \approx \mathrm{e}^{-A}. \tag{4.24}$$

This fluctuation occurs in spatial volume of order ℓ^3 on a timescale of about τ, so the corresponding rate per unit volume of vacuum decay by this mechanism is of order

$$\Gamma_{\bar{\dot{\phi}}} \approx \frac{1}{\tau\ell^3}\mathrm{e}^{-A}. \tag{4.25}$$

This is to be compared with the result in the instanton approximation, Eq. (2.12).

1. Thin wall case

Here we wish to compare estimates of A with B in the thin wall approximation. Take the example of the potential given in Eq. (2.3) for the case $\epsilon \ll 1$. To lowest order in ϵ, we have

$$\phi_F \approx a, \qquad \phi_0 \approx 0, \quad \text{and} \quad \Delta U \approx \frac{1}{8}\lambda a^4, \tag{4.26}$$

leading to

$$\dot{\phi}_0 \approx \frac{1}{2}\sqrt{\lambda}a^2, \tag{4.27}$$

and

$$\tau_0 \approx \frac{2}{\sqrt{\lambda}a}. \tag{4.28}$$

Note that $\tau_0 \approx 2/m$, where m given in Eq. (2.7), is the mass associated with the false vacuum state, and hence τ_0 is of the order of the period of harmonic field oscillations in the false vacuum. If we combine these estimates with $\ell_0 \approx \rho_{0tw}$ and Eq. (2.15), we find

$$A \approx \frac{4V^2L^3T}{\eta\epsilon^3\lambda}. \tag{4.29}$$

Comparison with Eq. (2.16) shows that $A < B$, and hence $\mathrm{e}^{-A} > \mathrm{e}^{-B}$, if

$$\frac{\eta}{V^2L^3T} > \frac{3}{2\pi^2} \approx 0.15. \tag{4.30}$$

The value of η depends upon the choices of the sampling functions $f(t)$ and $g(\mathbf{x})$, but can be expected to be of order one, in which case Eq. (4.30) will be satisfied if V^2L^3T is not too large.

However, comparison of the decay rate due to instanton effects, Γ_I and that due to $\bar{\dot{\phi}}$ fluctuations, $\Gamma_{\bar{\dot{\phi}}}$, also requires comparisons of the prefactors to the exponentials. Consider the case $T = L = 1$ and use Eqs. (2.15), (4.21), and (4.28) to find the $\Gamma_{\bar{\dot{\phi}}}$ prefactor to be

$$\frac{1}{\tau\ell^3} \approx \frac{1}{16}\epsilon^3\lambda^2a^4. \tag{4.31}$$

By contrast, the prefactor K, given in Eq. (2.22) is larger by a factor of order $\epsilon^{-10}\lambda^{-2}$, so instanton effects will dominate

if $A = B$. However, if $A < B$, a relatively small fractional difference can cause $\bar{\dot{\phi}}$ fluctuations to dominate. This will be illustrated in the next subsection.

2. Numerical simulations

Here we describe some numerical integrations of Eq. (3.1) with $U(\phi)$ as given in Eqs. (2.3) and (2.4). The initial condition is that $\phi(0) = \phi_+$, the false vacuum value, everywhere and that $\dot{\phi}(0)$ is a negative constant within a sphere of initial radius ℓ. The numerical solution, $\phi(t, r)$ is inspected to check that at least the region near $r = 0$ has passed through $\phi = \phi_m$ and reached $\phi \approx \phi_-$. If so, this describes a bubble of true vacuum surrounded by false vacuum formed by a $\bar{\dot{\phi}}$ fluctuation. However, a quantum fluctuation is transient and its energy must be given up on some timescale $\tau = T\tau_0$. We model this effect by stopping the numerical integration at $t = \tau$, and then restarting it with a new initial condition that $\phi(t = \tau, r)$ has the value found in the previous part of the integration, but $\dot{\phi}(t = \tau, r) = 0$. That is, the value of $\dot{\phi}$ is set to zero for the beginning of the second part of the simulation. Equation (3.1) is now further integrated with these initial conditions at $t = \tau$ to see if the bubble continues to expand.

The first part of the simulation for the case $L = 1.5$, $T = 1.25$, and $V = 1.5$ is illustrated in Fig. 3, and the second part in Fig. 4. The vertical plane in Fig. 3 corresponds to $t = \tau = 1.25\tau_0$, when the first part ends. By this time, the center of the bubble is in the true vacuum phase. Figure 4 illustrates the bubble expanding at close to the speed of light, with true vacuum in the interior, and false vacuum on the exterior.

For some choices of the parameters, the bubble fails to expand in the second part of the simulation, but rather collapses. Here the internal pressure due to the true vacuum energy is unable to overcome the wall tension. One such case is illustrated in Fig. 5.

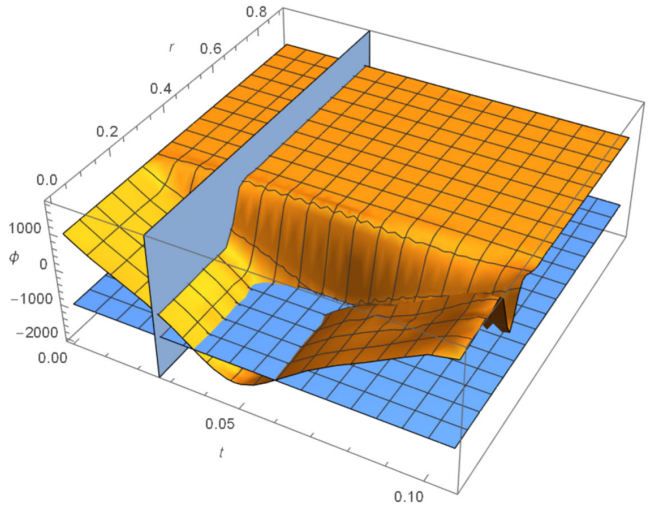

FIG. 3. The first part of the simulation, for the fluctuation in the case $L = 1.5$, $T = 1.25$, $V = 1.5$.

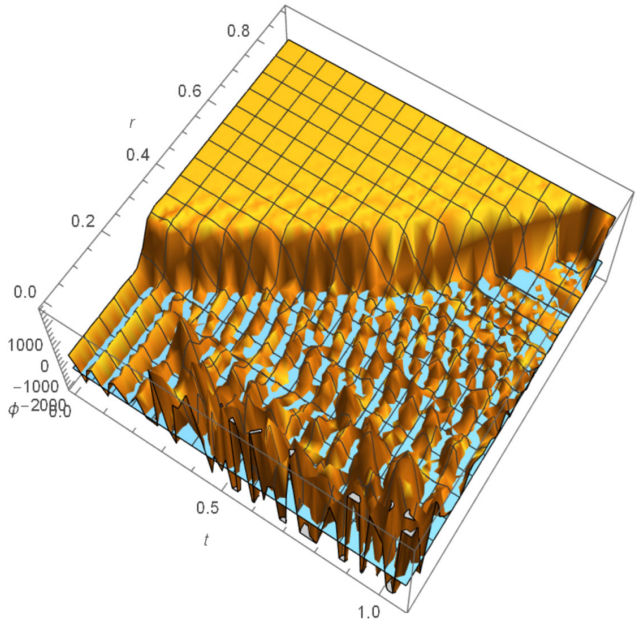

FIG. 4. The succeeding second part of the simulation, following Fig. 3.

Table I lists the results found with several choices of the parameters L, T, and V, along with the values of A and A/B. Here we have taken the temporal and spatial sampling functions to be given by Eqs. (4.16) and (4.17), respectively, and then numerically computed their Fourier transforms. These results are used in Eq. (4.9) to find value of η, which in turn is used to find A from Eq. (4.23). We also use

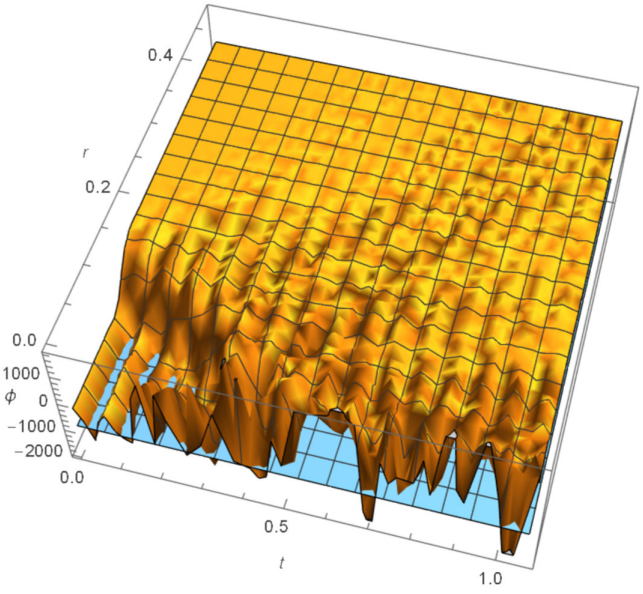

FIG. 5. The second step of the simulation for the case $L = 0.8$; $T = 1.25$; $V = 1.5$. The region of true vacuum fails to expand out.

TABLE I. The comparison between the two mechanisms of vacuum decay, for the potential barrier of $\lambda = 0.01$, $a = 1000$, $\epsilon = 0.1$, under different fluctuations.

L	T	V	$m\ell$	$m\tau$	η	A	A/B	Expand out?
1.5	1.25	1.5	27.518	2.43893	0.431466	5.90252×10^6	2.38785	Yes
1.4	1.25	1.5	25.6835	2.43893	0.430821	4.80616×10^6	1.94432	Yes
1.3	1.25	1.5	23.8489	2.43893	0.43002	3.85524×10^6	1.55963	Yes
1.2	1.25	1.5	22.0144	2.43893	0.429011	3.03938×10^6	1.22957	Yes
1.1	1.25	1.5	20.1799	2.43893	0.427715	2.34819×10^6	0.949954	Yes
1	1.25	1.5	18.3453	2.43893	0.426012	1.77128×10^6	0.716567	Yes
0.9	1.25	1.5	16.5108	2.43893	0.423715	1.29827×10^6	0.52521	Yes
0.9	1.25	1.5	16.5108	2.43893	0.423715	1.29827×10^6	0.52521	Yes
0.8	1.25	1.5	14.6763	2.43893	0.420515	918753.	0.371679	no
0.7	1.25	1.5	12.8417	2.43893	0.415878	622355.	0.251772	no
0.6	1.25	1.5	11.0072	2.43893	0.408819	398688.	0.161288	no

Eqs. (2.4), (2.5), (4.19), and (4.20), and $\ell_0 = 0.2$. Note that the thin wall approximation is not used here in the calculations of B.

In general, A/B is roughly of order unity, indicating roughly comparable contributions from $\bar{\dot{\phi}}$ fluctuations and from quantum tunneling in the instanton approximation to $\ln\Gamma$, the logarithm of the decay rate. The ratio of the prefactors in Γ_I and $\Gamma_{\bar{\dot{\phi}}}$ is of order

$$\tau\ell^3 K = \frac{2^9\pi^2}{9\sqrt{3}}\epsilon^{-10}\lambda^{-2} \approx e^{5.78-10\ln\epsilon-2\ln\lambda}, \quad (4.32)$$

where we have used Eqs. (2.22) and (4.31). In the present calculations, where $\epsilon = 0.1$ and $\lambda = 0.01$, this ratio becomes about $3.2 \times 10^{16} \approx e^{38}$, so the ratio of the decay rates is

$$\frac{\Gamma_I}{\Gamma_{\bar{\dot{\phi}}}} \approx e^{A-B+38}. \quad (4.33)$$

Although

However, although A/B is of order one, the magnitudes of A and B are sufficiently large that $|A - B + 38| \approx |A - B| \gg 1$, so the ratio of rates in Eq. (4.33) is either very large, as in the first four rows of Table I, or very small, as in the final six rows. In the former cases, quantum tunneling dominates, and the latter, $\bar{\dot{\phi}}$ fluctuations dominate.

D. Anticorrelated fluctuations

As noted above, we expect that the energy borrowed by the classical field from the quantum vacuum will tend to be returned on a timescale of order τ. This corresponds to the end of the first part of the simulations described in Sec. IV C 2 and illustrated in Fig. 3, and arises from the tendency of vacuum fluctuations to be anticorrelated. This effect was discussed in Refs. [34,35], where a correlation function was used to show that a typical fluctuation of quantities such as energy density or electric field tends to be followed by a fluctuation with the opposite sign. Here a typical fluctuation means one whose squared magnitude is of the order of the variance, σ^2. This anticorrelation acts to enforce energy conservation in a free field theory on a long timescale. Note from Eqs. (4.3) and (4.8), the probability $P(\bar{\dot{\phi}})$ decreases rapidly as τ increases for fixed $\bar{\dot{\phi}}$ and ℓ. This arises from the anticorrelations, which make it more difficult to observe a given value of $\bar{\dot{\phi}}$ over a longer averaging timescale. Note, however, that the effect of the original fluctuation is not guaranteed to be exactly canceled on any finite timescale. The analysis using correlation functions in Refs. [34,35] shows that on timescales a few times that associated with the original fluctuation, cancellation is just somewhat more likely than noncancellation.

This raises the question of whether an antifluctuation is likely to undo the effect of the initial large $\dot{\phi}$ fluctuation, and send the system back over the barrier to the false vacuum state after it has reached the true vacuum state. We argue that such an antifluctuation is unlikely. First, the arguments for anticorrelated fluctuations given in Refs. [34,35] rely upon an operator correlation function, or two-point function. The large fluctuations, large compared to the variance, are described by higher moments of the operator, or by n-point functions with $n \gg 1$. It is not clear if large fluctuations will soon be followed by equally large antifluctuations. Even if they are, there would be a limited time window for the antifluctuation to return the system to the false vacuum state. Once a bubble of true vacuum has formed and begun to expand rapidly, it is unlikely that an antifluctuation could stop this essentially classical expansion. The most that one can expect of the antifluctuation is that it takes back the energy borrowed from the quantum field by the original fluctuation. Once the bubble has begun to expand, its energy quickly becomes much larger than this value, and the bubble becomes a classical field configuration.

V. VACUUM DECAY INDUCED BY QUADRATIC OPERATOR FLUCTUATIONS

A. Probability distributions

In the previous section, we discussed the possibility that vacuum fluctuations of a linear operator, such as the spacetime average of $\dot{\phi}$, could induce decay of the false vacuum. Now we turn to the effects of the fluctuations of a quadratic operator, such as $\dot{\phi}^2$. The probability distributions for such operators have been treated in Refs. [17–21]. Just as is the case for $\dot{\phi}$, a quadratic operator must also be averaged in spacetime before a meaningful probability distribution can be defined. Recall that for a linear operator, the averaging could be over only time or only space, although we selected averaging in both as being more physically realistic. The averaging of a quadratic operator must be in time, as spatial averaging alone does not suffice. As before, we consider a spacetime average. A key result is that the probability distribution for an averaged quadratic operator, such as $\overline{\dot{\phi}^2}$, falls more slowly than exponentially for large fluctuations. This means that large fluctuations of $\overline{\dot{\phi}^2}$ and similar operators are more likely than one might expect, and hence may have larger physical effects than linear operator fluctuations.

Consider the case of a space and time average of normal ordered $:\dot{\phi}^2:$,

$$\overline{\dot{\phi}^2} = \int dt\, f(t) \int d^3x\, g(\mathbf{x}) :\dot{\phi}^2(\mathbf{x}, t):, \tag{5.1}$$

where we again take $f(t)$ and $g(\mathbf{x})$ to be functions with compact support whose Fourier transforms have the asymptotic forms given in Eq. (4.14). It is shown in Ref. [20] that when $\lambda \leq \alpha < 1$, the probability distribution and the complementary cumulative distribution functions for $\overline{\dot{\phi}^2}$ have the asymptotic forms,

$$P(\overline{\dot{\phi}^2}) \sim P_>(\overline{\dot{\phi}^2}) \sim \exp[-a_1(\tau^4 \overline{\dot{\phi}^2})^\alpha], \tag{5.2}$$

when $\ell \lesssim \tau$, and

$$P(\overline{\dot{\phi}^2}) \sim P_>(\overline{\dot{\phi}^2}) \sim \exp[-a_2(\ell^4 \overline{\dot{\phi}^2})^\alpha], \tag{5.3}$$

when $\ell \gtrsim \tau$. Here a_1 and a_2 are constants of order unity. Note that both $\tau^4\overline{\dot{\phi}^2}$ and $\ell^4\overline{\dot{\phi}^2}$ are dimensionless measures of the magnitude of $\overline{\dot{\phi}^2}$. The above asymptotic forms hold when the arguments of the exponentials are large compared to one. As in Sec. IV A, we are assuming that logarithm terms inside the exponentials are subdominant.

Note that it is the parameter α associated with $f(t)$ which governs the probability of large fluctuations. Because $\alpha < 1$, comparison of Eq. (4.3) with either of Eq. (5.2) or Eq. (5.3) shows that the probability of a large $\overline{\dot{\phi}^2}$ fluctuation can be much greater than that of the corresponding $\bar{\dot{\phi}}$ fluctuation for which $\bar{\dot{\phi}}^2 = \overline{\dot{\phi}^2}$.

The asymptotic probability distributions given in Eqs. (5.2) and (5.3) apply to other quadratic operators with the same dimensions as $\dot{\phi}^2$, including components of the stress tensor. Large radiation pressure fluctuations were discussed in Ref. [3], where it was argued that they can sometimes give a significant contribution to the barrier penetration rate of quantum particles. However, this requires especially small values of the switching parameter, $\alpha \lesssim 1/3$. For larger values of α, the radiation pressure fluctuation contribution is small compared to the barrier penetration rate found in the WKB approximation. It is important to note that the results summarized here are for $3+1$ dimensions. A $1+1$ dimensional model was treated in Ref. [36], and the probability distribution was found to fall more rapidly than in $3+1$ dimensions.

B. Effects of large $\overline{\dot{\phi}^2}$ fluctuations

We argued in Sec. IV C that the vacuum fluctuations of $\bar{\dot{\phi}}$ can produce a contribution to false vacuum decay which is comparable to the instanton contribution. Further, we have just seen that the probability of a $\overline{\dot{\phi}^2}$ fluctuation can be much larger than that of a comparable $\bar{\dot{\phi}}$ fluctuation, for which $(\bar{\dot{\phi}})^2 \approx \overline{\dot{\phi}^2}$. However, the possible effects of the two types of fluctuations are potentially very different. In Sec. IV C, we treated the effect of a large $\bar{\dot{\phi}}$ fluctuation as giving an initial condition for integration of the classical equation of motion for a self-coupled scalar field. We cannot expect that a large $\overline{\dot{\phi}^2}$ fluctuation will generally be accompanied by a comparable $\bar{\dot{\phi}}$ fluctuation. It is more likely that a large $\overline{\dot{\phi}^2}$ fluctuation will increase the energy of a finite region without necessarily changing the mean value of the classical scalar field significantly. This is similar to thermal fluctuations, which satisfy a Boltzmann probability distribution and can be described by a sphaleron [37,38]. Here a thermal fluctuation causes a finite region to go over the potential barrier.

However, if the mean value of the classical scalar field remains constant, then this region would seem to return to the false vacuum state when the $\overline{\dot{\phi}^2}$ fluctuation has finished. One way to avoid this would be a simultaneous $\bar{\dot{\phi}}$ fluctuation which pushes the region over the potential maximum, so that it ends in the true vacuum state. The effects of both fluctuations are illustrated in Fig. 6. In principle, the timescales of the two fluctuations could be different, but here we assume that they are of the same order.

The minimal $\overline{\dot{\phi}^2}$ fluctuation needed raise the region above the potential maximum has a magnitude of

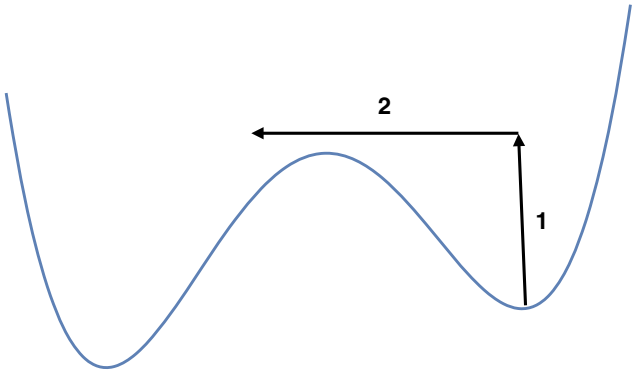

FIG. 6. Here the combined effects of a large $\overline{\dot{\phi}^2}$ fluctuation (Step 1), and a subsequent $\bar{\dot{\phi}}$ fluctuation (Step 2) are illustrated.

$\overline{\dot{\phi}^2} \approx 2\Delta U$, where ΔU is the potential difference defined in Eq. (4.18). If $\ell \gtrsim \tau$ and we set $a_2 \approx 1$, in Eq. (5.3), the probability of the required $\overline{\dot{\phi}^2}$ fluctuation is of order

$$P_1(\overline{\dot{\phi}^2}) \approx P_>(\overline{\dot{\phi}^2}) \approx \exp[-(2\ell^4 \Delta U)^\alpha]. \tag{5.4}$$

Here the subscript 1 refers to the first step in Fig. 6, and we assume that $(2\ell^4\Delta U)^\alpha \gg 1$, so that Eq. (5.3) holds. We may view a positive $\overline{\dot{\phi}^2}$ fluctuation as raising the average energy density, and hence the energy E_R, defined in Eq. (3.3), of the region.

The second step, denoted by the label 2 in Fig. 6, involves a linear field fluctuation, similar to those treated in Sec. IV C. However, now we may treat the field as approximately massless, and assume that Eq. (4.11) holds if $\ell \gtrsim \tau$. In this case, the probability of a large $\bar{\dot{\phi}}$ fluctuation is approximately

$$P_2(\bar{\dot{\phi}}) \approx P_>(\bar{\dot{\phi}}) \approx \exp(-\ell^4 \bar{\dot{\phi}}^2). \tag{5.5}$$

However, unlike in Sec. IV C, now the $\bar{\dot{\phi}}$ fluctuation does not need to raise a region from the false vacuum minimum over the potential barrier, but rather simply has to translate by $\Delta\phi$ in a time τ, the duration of the $\overline{\dot{\phi}^2}$ fluctuation in step 1. Thus we require

$$|\bar{\dot{\phi}}| \geq \frac{|\Delta\phi|}{\tau} \approx \frac{a}{\tau}. \tag{5.6}$$

In writing Eq. (5.4), we assumed that $\ell \gtrsim \tau$ and obtained a result which does not explicitly depend upon τ. This means that a typical $\overline{\dot{\phi}^2}$ fluctuation may be assumed to last for a time which is of the order of ℓ. For an estimate, we set $\tau \approx \ell$ in Eq. (5.6) and write

$$P_2(\bar{\dot{\phi}}) \approx \exp(-\ell^2 a^2). \tag{5.7}$$

Now we need the probability of the $\overline{\dot{\phi}^2}$ fluctuation and the $\bar{\dot{\phi}}$ fluctuation together, which depends upon whether the two fluctuations are correlated. In lowest order, they are not, as $\langle \bar{\dot{\phi}}\, \overline{\dot{\phi}^2} \rangle = 0$. However, there is a possibility of higher order correlations. Here we assume that the two fluctuations are uncorrelated, so the probability of the two-step process depicted in Fig. 6 is

$$P_{12} = P_1(\overline{\dot{\phi}^2}) P_2(\bar{\dot{\phi}}). \tag{5.8}$$

The decay rate per unit volume will again be taken to be

$$\Gamma_2 = \frac{P_{12}}{\tau \ell^3} \tag{5.9}$$

as in Eq. (4.25). Note that the anticorrelations discussed in Sec. IV D occur for the same operator measured at different times, and are not directly relevant here.

Now we wish to make some estimates of P_{12}. Consider the case $\alpha = 1/2$ and assume the thin wall approximation, so $\epsilon \ll 1$. We also assume that the spatial averaging scale is of the order of the initial bubble radius given in Eq. (2.15), so

$$\ell \approx \frac{2}{\epsilon a \sqrt{\lambda}}. \tag{5.10}$$

We may combine this with Eq. (4.26) to write

$$P_1(\overline{\dot{\phi}^2}) \approx \exp\left(-\frac{2}{\epsilon^2\sqrt{\lambda}}\right). \tag{5.11}$$

Similarly, we find

$$P_2(\bar{\dot{\phi}}) \approx \exp\left(-\frac{4}{\epsilon^2\lambda}\right). \tag{5.12}$$

Note that here $P_2(\bar{\dot{\phi}})$ is much larger than the probability of the $\bar{\dot{\phi}}$ fluctuations considered in Sec. II, as the magnitude of the $\bar{\dot{\phi}}$ fluctuation considered here is much smaller than that needed to lift a region over the barrier.

Now we have

$$P_{12} = \mathrm{e}^{-C} \tag{5.13}$$

where

$$C \approx \frac{2}{\epsilon^2\lambda}(2 + \sqrt{\lambda}). \tag{5.14}$$

Comparison with Eq. (2.16) reveals

$$\frac{C}{B_{tw}} = \frac{3\epsilon}{4\pi^2}(2+\sqrt{\lambda}), \tag{5.15}$$

$C < B$ in the thin wall approximation ($\epsilon \ll 1$), unless λ is very large. Then the combined effects of $\overline{\dot{\phi}^2}$ and $\bar{\dot{\phi}}$ fluctuations might dominate quantum tunneling. This conclusion depends upon the assumption that the $\overline{\dot{\phi}^2}$ and $\bar{\dot{\phi}}$ fluctuations are uncorrelated, or at least not strongly anticorrelated. This assumption needs further investigation.

Under this assumption, we may write the ratio of the decay rate due to tunneling to that due to fluctuations as

$$\frac{\Gamma_I}{\Gamma_2} \approx \mathrm{e}^{C-B+5.78-10\ln\epsilon-2\ln\lambda}. \tag{5.16}$$

In the limit of small ϵ for fixed λ, this ratio approaches $\mathrm{e}^{-B} \ll 1$, so fluctuations give the dominant contribution to the decay rate.

C. Measurement of $\overline{\dot{\phi}^2}$

In this subsection, we will describe a thought experiment by which an averaged quadratic operator such as $\overline{\dot{\phi}^2}$ could be measured in a compact region of spacetime. Consider the Raychaudhuri equation for the expansion θ of a bundle of timelike geodesics:

$$\frac{d\theta}{d\tau} = -R_{\mu\nu}u^\mu u^\nu, \tag{5.17}$$

where $R_{\mu\nu}$ is the Ricci tensor, u^μ is the four-velocity of a particle on a geodesic, and τ is its proper time. Here we have assumed that terms involving θ^2 or the squares of the shear or vorticity may be neglected. If we measure the change in the expansion of the bundle, $\Delta\theta$, averaged over finite intervals of time and space, then we have measured certain components an averaged Ricci tensor, $\overline{R_{\mu\nu}}$, averaged with compactly supported sampling functions $f(t)$ and $g(\mathbf{x})$ defined by the details of the geodesic bundles. By varying the four-velocity, u^μ, we can potentially obtain all of the diagonal components of $\overline{R_{\mu\nu}}$. Next we may infer the averaged components of the stress tensor from the Einstein equation in the form

$$\overline{T_{\mu\nu}} = \frac{1}{8\pi G}\left(\overline{R_{\mu\nu}} - \frac{1}{2}g_{\mu\nu}\bar{R}\right), \tag{5.18}$$

where G is Newton's constant and $R = R^\mu{}_\mu$.

Now we assume that the source of the gravitational field is the self-coupled scalar field with Lagrangian density given in Eq. (2.1), for which the stress tensor is

$$T_{\mu\nu} = \partial_\mu\phi\partial_\nu\phi - \frac{1}{2}g_{\mu\nu}\partial^\rho\phi\partial_\rho\phi - g_{\mu\nu}U(\phi). \tag{5.19}$$

Further assume that the gravitational field is weak, and that in the above expression we may take the metric to have the Minkowski form $g_{\mu\nu} \approx \eta_{\mu\nu} = \mathrm{diag}(-1,1,1,1)$. If we form a particular combination of the components of $T_{\mu\nu}$, the potential $U(\phi)$ cancels, and we have

$$3T_{tt} + T_{xx} + T_{yy} + T_{zz} = 3\dot{\phi}^2 + |\boldsymbol{\nabla}\phi|^2. \tag{5.20}$$

We expect $\dot{\phi}^2$ and $|\boldsymbol{\nabla}\phi|^2$ to be of the same order of magnitude, so measurements of $\overline{R_{\mu\nu}}$, and hence of $\overline{T_{\mu\nu}}$, allow us to obtain an estimate of $\overline{\dot{\phi}^2}$.

D. What determines α?

We have seen that the probability distributions for the fluctuations of quadratic operators, such as $\overline{\dot{\phi}^2}$, are very sensitive to the parameter α defined in Eq. (4.14). This parameter determines the rate of decrease of $\hat{f}(\omega)$, the Fourier transform of the temporal sampling function $f(t)$, and is also linked to the switch-on and switch-off behavior of $f(t)$. In the measurement of $\overline{\dot{\phi}^2}$ described in the previous subsection, α will be determined by the details of the bundles of test particles used. The more rapidly these bundles begin and end, the smaller will be α, and hence the larger the likely value of $\overline{\dot{\phi}^2}$ obtained in the measurement. This seems to imply that if we measure $\overline{\dot{\phi}^2}$ in the false vacuum state with bundles with small α, the probability of immediate decay is much greater than if we had use a larger value of α. This issue needs further study, as it is not immediately clear why a purely gravitational measurement should perturb the scalar field theory so much.

Another open question is what effect will fluctuations have upon the false vacuum in the apparent absence of a measurement of the form described above. It is possible that the dynamics of coupling of the quantum field fluctuations with the classical background scalar field can determine a specific value of α, but how this might happen is unclear.

E. Comparison of the effects of scalar and electromagnetic field fluctuations

Recall that quantum electric field fluctuations have a small effect, of the order of 1%, on the rate of quantum tunneling of electrons through a potential barrier [1,2]. In contrast, we found in Sec. IV C that the effects of $\dot{\phi}$ fluctuations can be comparable to the rate of false vacuum decay as calculated in the instanton approximation, essentially a relative contribution of $O(1)$. We can understand this difference as arising from the weakness of the electromagnetic interaction. The electric field fluctuation effect is a one-loop correction to the tunneling rate, and is suppressed by a factor of the fine structure constant.

Similarly, the contribution of radiation pressure fluctuations to charged particle tunneling is very sensitive to the

switching parameter α, and will be small compared to the WKB contribution unless $\alpha \lesssim 1/3$ [3]. By contrast, we argued above that $\overline{\dot{\phi}^2}$ fluctuations can give an $O(1)$ contribution to false vacuum decay.

As discussed in Sec. II A, the instanton approximation seems to give a good description of the Schwinger effect in both $1+1$ and $3+1$ dimensions. However, the possible role of vacuum radiation pressure fluctuations in the latter case merits further study. The Schwinger effect may be viewed as charged particle tunneling, so one expects the contributions of both quantum electric field fluctuations and of radiation pressure fluctuations to be small. Thus one cannot use the agreement of instanton and Bogolubov coefficient methods in the Schwinger effect to infer that $\bar{\dot{\phi}}$ or $\overline{\dot{\phi}^2}$ fluctuations will give a small contribution to false vacuum decay.

VI. SUMMARY AND CONCLUSIONS

In this paper, we have discussed the effects of linear and quadratic quantum field fluctuations on the decay rate of a false vacuum of a self-coupled scalar field. This rate is usually computed in an instanton approximation, where the solution of lowest Euclidean action is assumed to dominate a path integral. We first consider the effects of the vacuum fluctuations of a linear field, $\dot{\phi}$, averaged over finite intervals of both space and time. We have argued that this averaging describes a physical process or measurement which necessarily begins and ends at finite times, and occurs in compact regions of space and time. Hence the averaging should be described by infinitely differentiable, but compactly supported and hence non-analytic functions of space and time. A quantum $\dot{\phi}$ fluctuation in a finite region has an effect similar to a classical initial field velocity, and if its magnitude is large enough, can cause a finite region to fly over a potential barrier, in a manner similar to the motion of a classical particle.

We find that quantum $\dot{\phi}$ fluctuations can cause false vacuum decay at a rate which can be comparable to the rate of quantum tunneling, as described in the instanton approximation. This is consistent with the conclusions in Refs. [6–11,13–16], although these authors offer differing conclusions as to whether linear quantum field fluctuations are an alternative formalism for describing quantum tunneling, or represents a distinct physical process. We adopt the latter viewpoint. Evidence that $\dot{\phi}$ fluctuations are a separate decay channel from tunneling arises in the wide variation in decay rates, as opposed to the logarithm of the rates found in Sec. IV C 2. Further evidence comes from the dependence of the variance in Eqs. (4.8) and (4.9) upon the sampling functions. Our view is that these functions should be determined by the physical details of the system, here perhaps the dynamics of the formation of the bubble of true vacuum.

This dependence is even more pronounced in the case of the effects of quadratic quantum field fluctuations, such as $\overline{\dot{\phi}^2}$, upon the decay rate. Here we found an effect which can be significantly more likely than large $\bar{\dot{\phi}}$ fluctuations. This arises because the probability distribution, $P(\overline{\dot{\phi}^2})$, falls more slowly than an exponential function when compactly supported averaging functions are used, and provides evidence that both $\bar{\dot{\phi}}$ and $\overline{\dot{\phi}^2}$ fluctuations provide different decay processes than quantum tunneling. However, our analysis in Sec. V B relies upon an assumption, Eq. (5.8), concerning the correlation of linear and quadratic operator fluctuations which need to be examined further. If this assumption is correct, then at least for false vacuum decay in $3+1$ dimensions, quadratic operator fluctuations may be the dominant decay mechanism. The role of such fluctuations in other contexts remains to be explored in more detail.

ACKNOWLEDGMENTS

We would like to thank Mark Hertzberg, Ken Olum, Alex Vilenkin, Shao-Jiang Wang, and Masaki Yamada for helpful discussions. We also thank Ali Masoumi for providing the software package described in Ref. [32], and for assistance in its use. This work was supported in part by the National Science Foundation under Grant No. PHY-1912545.

[1] V. V Flambaum and V. G. Zelevinsky, Radiation Corrections Increase Tunneling Probability, Phys. Rev. Lett. **83**, 3108 (1999).
[2] H. Huang and L. H. Ford, Quantum electric field fluctuations and potential scattering, Phys. Rev. D **91**, 125005 (2015).
[3] H. Huang and L. H. Ford, Vacuum radiation pressure fluctuations and barrier penetration, Phys. Rev. D **96**, 016003 (2017).
[4] L. H. Ford, Vacuum radiation pressure fluctuations on atoms, Phys. Rev. A **104**, 012208 (2021).
[5] S. Coleman, Fate of the false vacuum: Semiclassical theory, Phys. Rev. D **15**, 2929 (1977).
[6] A. Linde, Stochastic approach to tunneling and baby universe formation, Nucl. Phys. **B372**, 421 (1992).
[7] E. Calzetta and E. Verdaguer, Noise induced transitions in semiclassical cosmology, Phys. Rev. D **59**, 083513 (1999).

[8] E. Calzetta, A. Roura, and E. Verdaguer, Dissipation, Noise and Vacuum Decay in Quantum Field Theory, Phys. Rev. Lett. **88**, 010403 (2001).
[9] E. Calzetta, A. Roura, and E. Verdaguer, Vacuum decay in quantum field theory, Phys. Rev. D **64**, 105008 (2001).
[10] D. Arteaga, E. Calzetta, A. Roura, and E. Verdaguer, Activation-like processes at zero temperature, Int. J. Theor. Phys. **42**, 1257 (2003).
[11] E. Calzetta and E. Verdaguer, Real time approach to tunneling in open quantum systems: Decoherence and anomalous diffusion, J. Phys. A **39**, 9503 (2006).
[12] H. Huang, False vacuum decay and quantum fluctuations, seminar at Tufts University, (2018).
[13] J. Braden, M. C. Johnson, H. V. Peiris, A. Pontzen, and S. Weinfurtner, A New Semiclassical Picture of Vacuum Decay, Phys. Rev. Lett. **123**, 031601 (2019).
[14] M. P. Hertzberg and M. Yamada, Vacuum decay in real time and imaginary time formalisms, Phys. Rev. D **100**, 016011 (2019).
[15] J. J. Blanco-Pillado, H. Deng, and A. Vilenkin, Flyover vacuum decay, J. Cosmol. Astropart. Phys. 12 (2019) 001.
[16] S.-J. Wang, Occurrence of semiclassical vacuum decay, Phys. Rev. D **100**, 096019 (2019).
[17] C. J. Fewster, L. H. Ford, and T. A. Roman, Probability distributions for quantum stress tensors in four dimensions, Phys. Rev. D **85**, 125038 (2012).
[18] C. J. Fewster and L. H. Ford, Probability distributions for quantum stress tensors measured in a finite time interval, Phys. Rev. D **92**, 105008 (2015).
[19] E. D. Schiappacsse, C. J. Fewster, and L. H. Ford, Vacuum quantum stress tensor fluctuations: A diagonalization approach, Phys. Rev. D **97**, 025013 (2018).
[20] C. J. Fewster and L. H. Ford, Probability distributions for space and time averaged quantum stress tensors, Phys. Rev. D **101**, 025006 (2020).
[21] P. Wu, L. H. Ford, and E. D. Schiappacasse, Space and time averaged quantum stress tensor fluctuations, Phys. Rev. D **103**, 125014 (2021).
[22] S. Coleman, *Aspects of Symmetry* (Cambridge University Press, Cambridge, England, 1985), Chap. 7.
[23] G. V. Dunne and K. Rao, Lamé Instantons, J. High Energy Phys. 01 (2000) 019.
[24] H. J. W. Müller-Kirsten, J.-z. Zhang, and Y. Zhang, Once again: Instanton method vs WKB, J. High Energy Phys. 11 (2001) 011.
[25] V. A. Benderskii, E. V. Vetoshkin, and E. I. Kats, Accuracy of semiclassics: Comparative analysis of WKB and instanton approaches, HAIT J. Sci. Eng. A **5**, 71 (2008), http://www.magniel.com/jse/A/vol0501/p71.html.
[26] J. Schwinger, Gauge invariance and vacuum polarization, Phys. Rev. **82**, 664 (1951).
[27] J. Garriga, Nucleation rates in flat and curved space, Phys. Rev. D **49**, 6327 (1994).
[28] S. P. Kim and D. N. Page, Schwinger pair production via instantons in strong electric fields, Phys. Rev. D **65**, 105002 (2002).
[29] J. Garriga, Pair production by an electric field in $(1+1)$-dimensional de Sitter space, Phys. Rev. D **49**, 6343 (1994).
[30] A. A. Grib, S. G. Mamayev, and V. M. Mostepanenko, *Vacuum Quantum Effects in Strong Fields* (Frienmann Laboratory Publishing, St. Petersberg, 1994), Chap. 4.
[31] C. G. Callan and S. Coleman, Fate of the false vacuum II: First quantum corrections, Phys. Rev. D **16**, 1762 (1977).
[32] A. Masoumi, K. Olum, and B. Shlaer, Efficient numerical solution to vacuum decay with many fields, J. Cosmol. Astropart. Phys. 01 (2017) 051.
[33] B. Garbrecht and P. Millington, Greens function method for handling radiative effects on false vacuum decay, Phys. Rev. D **91**, 105021 (2015).
[34] L. H. Ford and T. A. Roman, Minkowski vacuum stress tensor fluctuations, Phys. Rev. D **72**, 105010 (2005).
[35] V. Parkinson and L. H. Ford, A model for non-cancellation of quantum electric field fluctuations, Phys. Rev. A **84**, 062102 (2011).
[36] C. J. Fewster, L. H. Ford, and T. A. Roman, Probability distributions of smeared quantum stress tensors, Phys. Rev. D **81**, 121901 (2010).
[37] F. R. Klinkhamer and N. S. Manton, A saddle-point solution in the Weinberg-Salam theory, Phys. Rev. D **30**, 2212 (1984).
[38] P. Arnold and L. McLerran, Sphalerons, small fluctuations, and baryon-number violation in electroweak theory, Phys. Rev. D **36**, 581 (1987); The sphaleron strikes back: A response to objections to the sphaleron approximation, Phys. Rev. D **37**, 1020 (1988).